Nuclear Instruments and Methods in Physics Research B 377 (2016) 89–93

Contents lists available at ScienceDirect

Nuclear Instruments and Methods in Physics Research B

journal homepage: www.elsevier.com/locate/nimb

Evaluation of Ce:$SrAl_2O_4$ crystalline scintillators

Daisuke Nakauchi [a,*], Go Okada [a], Masanori Koshimizu [b], Takayuki Yanagida [a]

[a] Graduate School of Materials Science, Nara Institute of Science and Technology (NAIST), 8916-5 Takayama, Ikoma, Nara 630-0192, Japan
[b] Department of Applied Chemistry, Graduate School of Engineering, Tohoku University, 6-6-07 Aoba, Aramaki, Aoba, Sendai 980-8579, Japan

ARTICLE INFO

Article history:
Received 10 February 2016
Received in revised form 23 March 2016
Accepted 9 April 2016

Keywords:
Scintillation
Photoluminescence
Thermally stimulated luminescence
Optically stimulated luminescence
Strontium aluminate
Cerium
Single crystal

ABSTRACT

In this study, Ce-doped $SrAl_2O_4$ (Ce:$SrAl_2O_4$) crystals were prepared by a floating zone (FZ) method and experimental evaluations were performed for scintillator applications. In photoluminescence (PL) with an excitation around 320 nm, an intense broad emission peak appears around 380 nm due to the 5d-4f transitions. The PL decay time constants are approximately 30 ns. The X-ray induced scintillation spectrum also shows an intense broad emission peak around 380 nm. Among the samples evaluated with different concentrations of Ce, the absolute light yield under ^{137}Cs is considerably high (~3900 ph/MeV) when the concentration of Ce is 1.0%. In thermally stimulated luminescence (TSL) after X-ray irradiation, strong TSL glow peaks are observed at 110, 210 and 330 °C. The samples also shows optically stimulated luminescence (OSL) after X-ray irradiation, in which the emission appears around 380 nm due to the 5d-4f emission bands of Ce^{3+} while the samples is exposed to the stimulation light at 655 nm.

1. Introduction

Scintillating materials convert incident ionizing radiation such as high energy photons and particles to a large number of ultraviolet–visible photons immediately. Such scintillators play an important role for radiation detection applied in various fields, for example medical imaging [1], security [2], astrophysics [3] and geophysical and resources exploration, e.g. oil-dwelling [4]. Among these applications, especially scintillators for X-ray and γ-ray detectors have attracted considerable attentions since the market size of medical and security fields are large. A conventional radiation detector using a scintillator consists of a scintillator (to convert radiation to light) and photodetectors (to convert light to electronic signal). Such detection technique can be further classified into two types. One is based on a photon-counting (pulse height) technique and the other is based on signal integration. As a photodetector, photomultiplier tube (PMT) is a strong tool and often used since it has a very fast response and high quantum efficiency in the UV-blue region. Therefore, a scintillator to be used with a PMT is preferred to show UV-blue light emission.

The recent trend of developing new scintillator is based on a combination of insulator as a host and rare earth ion as emission center. Among such phosphors, Ce^{3+}-doped materials are one of the most common scintillator due to the strong optical absorption and emission in the near ultraviolet–visible region due to the parity and spin allowed electron transitions. The emission due to the 5d-4f transitions of Ce^{3+} is characterized by a broad emission band with relatively a longer wavelength than 5d-4f transitions of other rare earth elements (e.g., vacuum ultra violet (VUV) emission from Nd^{3+} [5]) and fast decay time of several tens of nanoseconds. Such fast scintillation is advantageous especially in positron emission tomography (PET), which requires radiation detection with high counting rate. Up to now, the most common Ce-doped scintillators are rare earth silicate materials [6–9], and many efforts have been paid to develop new Ce-doped scintillators.

To date, rare-earth doped $SrAl_2O_4$ have been widely studied in the fields of long persistent phosphors [10–15], and scintillation from $SrAl_2O_4$ co-doped with Eu and Dy in the nano powder or sintered ceramic forms has been also reported [16–20]. However, no studies have been reported for the scintillation properties of Ce-doped $SrAl_2O_4$ as far as we know. In addition, for typical scintillator uses, a bulk form is particularly important since the interaction probability of ionizing radiations with materials simply depends on the detector volume, so bulk crystalline scintillators are practically used except for some special applications.

In this study, we investigated the scintillation properties of undoped and Ce-doped $SrAl_2O_4$ (Ce:$SrAl_2O_4$) crystals with different Ce concentrations. In addition, we also study the dosimetric properties such as thermally stimulated luminescence (TSL) and optically stimulated luminescence (OSL) to comprehensively evaluate radiation induced luminescence properties since scintillation and

* Corresponding author.
E-mail address: nakauchi.daisuke.mv7@ms.naist.jp (D. Nakauchi).

http://dx.doi.org/10.1016/j.nimb.2016.04.017
0168-583X/© 2016 Published by Elsevier B.V.

dosimeter properties are complementary related [21]. Also, some defect centers are expected to be created when the Ce^{3+} ion substitutes the Sr^{2+} site as these valence states are different, and these centers may act charge trapping centers.

2. Experimental

Undoped and Ce-doped $SrAl_2O_4$ crystals were synthesized by a floating zone (FZ) method using the FZ furnace (FZD0192, Canon Machinery Inc.). We used $SrCO_3$ (4N), Al_2O_3 (4N), and CeO_2 (4N) powders as raw materials. The concentration of Ce varies as 0%, 0.5%, 1.0% and 2.0%, and the Ce dopant is externally introduced to the chemical composition of $SrAl_2O_4$. The starting compounds were mixed first, and the mixture was shaped in a cylinder form by the hydrostatic pressure. Then, the cylinder was sintered at 1500 °C for 6 h to obtain a $SrAl_2O_4$ ceramic rod. The sintered rod was loaded into the FZ furnace and the crystal growth was conducted with the translation rate of 5 mm/h and the rotation rate of 20 rpm. The heat source of the FZ furnace is halogen lamp. The synthesized sample was characterized by the measurements below.

The photoluminescence (PL) emission map and quantum yield (*QY*) were evaluated by using Quantaurus-QY (Hamamatsu Photonics). The PL decay time profile monitoring at 380 nm under 280 nm excitation was evaluated by using Quantaurus-τ (Hamamatsu Photonics). The decay time was deduced by the least square fitting of single exponential decay function. In addition, the excitation spectrum in near ultraviolet region was observed by using FP8600 spectrofluorometer (JASCO) while the excitation spectrum in the VUV range was measured at a synchrotron facility (UVSOR). The range of measured excitation wavelength in the VUV region was from 50 to 190 nm.

As a scintillation property, X-ray induced radioluminescence (RL) spectrum was measured by utilizing our original setup [22]. The irradiation source is an X-ray generator equipped with a tungsten anode target (XRB80P&N200X4550, Spellman). During the measurements, the X-ray generator was supplied with the bias voltage of 80 kV and tube current of 2.5 mA. While the sample was irradiated by X-rays, the RL emission from the sample was fed into the spectrometer through a 2 m optical fiber to measure the spectrum. The spectrometer (Andor DU-420-BU2 CCD with Shamrock SR163 monochromator) was cooled down to 188 K by a Peltier module to reduce the thermal noise. Further, we have measured the scintillation decay time and the afterglow profiles using a pulsed X-ray source equipped afterglow characterization system [23]. In both PL and scintillation decay time profiles, we fitted the data only in the tail part assuming a single exponential function. In the pulse height measurement, we mounted each crystal on the PMT (R877-100, Hamamatsu) with a silicon grease (6262A, OKEN), and the sample was covered by several layers of Teflon reflectors to guide scintillation photons to the PMT. Here, the scintillation light is converted to electronical signal by the PMT, which is then processed by the preamplifier (113, ORTEC), shaping-amplifier (572, ORTEC) with 0.5 μs shaping time and multichannel analyzer (AMPTEK Pocket MCA). The pulse height spectrum is eventually stored on a computer.

In order to characterize relatively shallow trapping centers, the thermally stimulated luminescence (TSL) glow curve was measured by TL-2000 (Nanogray, Japan) with the heating rate of 1 °C/s over the temperature range from 50 to 490 °C [24]. On the other hand, for deeper trapping centers, optically stimulated luminescence (OSL) was also studied under 655 nm stimulation by using FP8600 spectrofluorometer (JASCO). Except for the TSL, the sample for all the other measurements mentioned above was at room temperature.

3. Results and discussion

The synthesized undoped and Ce:$SrAl_2O_4$ crystals are shown in Fig. 1. Although no reports can be found for bulk shape, we could successfully obtain bulk crystalline samples with a typical sizes of 4–5 mm ϕ × 20–30 mm in length. Visibly they are white and translucent. Under UV lamp irradiation (254 nm), a bright blue luminescence due to the 5d-4f transition of Ce^{3+} can be seen by naked eye. We cut these crystalline rods to extract a relatively transparent part with a typical size of 4–5 mm ϕ × 2 mm for characterizations.

The PL emission and excitation map of 1.0% Ce:$SrAl_2O_4$ crystal is represented in Fig. 2. Under excitation around 320 nm, an intense broad emission around 380 nm is observed. This emission origin is attributed to the 5d-4f transition of Ce^{3+} from the past study in powder forms [13–15]. The *QY* of the 0.5%, 1.0% and 2.0% Ce:$SrAl_2O_4$ crystals upon excitation at 330 nm are 13%, 39% and 14%, respectively. In the undoped sample, no emissions can be detected. The 1.0% Ce-doped sample shows the best PL *QY* among the present samples.

The PL decay time profiles of the Ce:$SrAl_2O_4$ crystals are shown in Fig. 3. The decay time constants of the samples monitoring at 380 nm emission band upon 280 nm excitation are approximately 30 ns. These are almost the same as the typical time constants of 5d-4f transition of Ce^{3+} [15], and no slow component is detected in PL. In PL decay time profiles, no significant difference is observed in different Ce concentrations.

In order to investigate $5d_1$-$5d_5$ levels of Ce^{3+}, PL excitation spectra of the 1.0% Ce-doped sample monitoring at the 5d-4f emission of Ce^{3+} are displayed in Fig. 4. The monitoring wavelength at UVSOR was 400–410 nm which was the tail part of the emission (see Fig. 2) to avoid any influences of the diffraction light. Six excitation bands are observed, and the bands around 255, 280 and 325 nm are observed by former works [11,12]. These bands are ascribed to the 4f-$5d_{1\text{-}3}$ levels transitions of Ce^{3+}. In the VUV range, the excitation band around 180 nm would correspond to the transitions from between the top of valence band and bottom of conduction band since the band gap energy of $SrAl_2O_4$ is reported to be 6.5 eV (190 nm) [12]. Therefore, the remaining two bands, 120 and 150 nm will be assigned to 4f-$5d_{4\text{-}5}$ transitions. Therefore, the excitation bands around 120, 150, 255, 280 and 325 nm would be attributed to the 4f-$5d_{1\text{-}5}$ transitions of Ce^{3+} ($^2F_{5/2} \rightarrow {}^2D$).

The X-ray induced RL spectra are shown in Fig. 5. An intense broad emission peak around 380 nm is observed as the same for PL, so the emission origin is ascribed to the 5d-4f transition of Ce^{3+}. Compared with other famous Ce-doped scintillators, emission wavelength is similar to the scintillation from Ce-doped rare earth silicate materials [6,7], and shorter than Ce-doped garnet scintillators [22,25]. In the undoped sample, broad emission bands around 500 nm appear. The emission origin of the undoped sample is discussed in elsewhere based on luminescence properties under VUV photon excitations at Synchrotron facility, and we concluded the origin as the perturbed self-trapped exciton (STE) [26]. Although RL are qualitative evaluation since we cannot correct the stopping power of each scintillator material, the scintillation intensity of the undoped sample was significantly weaker than Ce-doped samples. By the Ce-doping, this STE based host emission is suppressed.

X-ray induced RL decay time profiles of the Ce:$SrAl_2O_4$ crystals are represented in Fig. 6. The decay curves consist of one exponential function, and the decay time constants of the 0.5%, 1.0% and 2.0% Ce-doped samples are 47.3, 48.0 and 51.7 ns, respectively. These are slightly slower than those in PL due to the difference of the energy migration processes of the PL and scintillation. In PL, we observe the direct excitation and de-excitation of energy levels of Ce^{3+} while the additional transportation process from the host to emission centers occurs in scintillation. In addition,

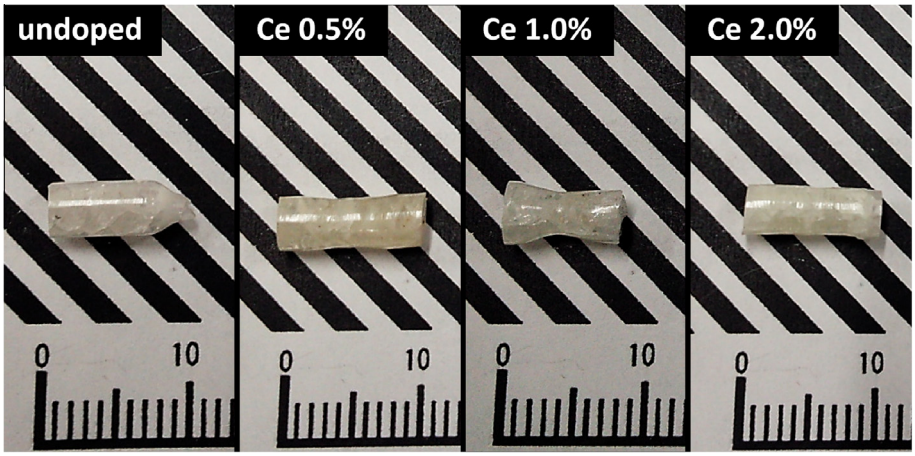

Fig. 1. Appearances of partly cut Ce:$SrAl_2O_4$ crystals synthesized by the FZ method.

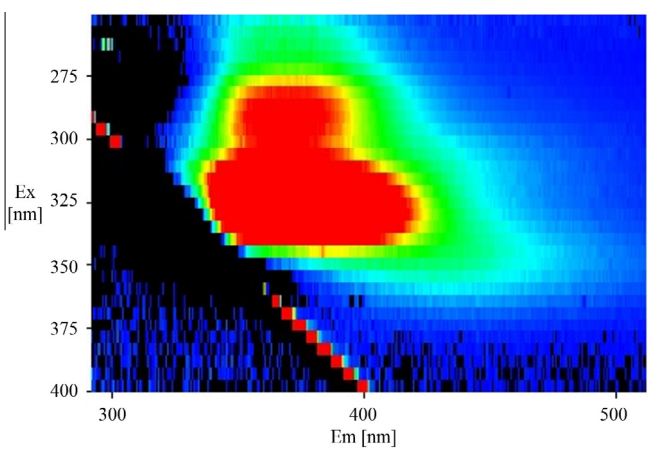

Fig. 2. PL emission and excitation map of the 1.0% Ce:$SrAl_2O_4$ crystal as a representative. The horizontal axis shows the emission and the vertical axis shows the excitation wavelengths, respectively.

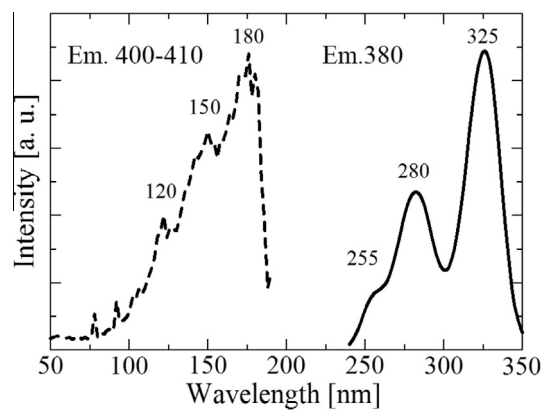

Fig. 4. PL excitation spectra of the 1.0% Ce:$SrAl_2O_4$ crystal monitoring at the 5d-4f emission of Ce^{3+}. The spectra in the VUV (dashed line) and near ultraviolet (solid line) were measured by Synchrotron facility (UVSOR) and common spectrofluorometer (FP8600, JASCO), respectively.

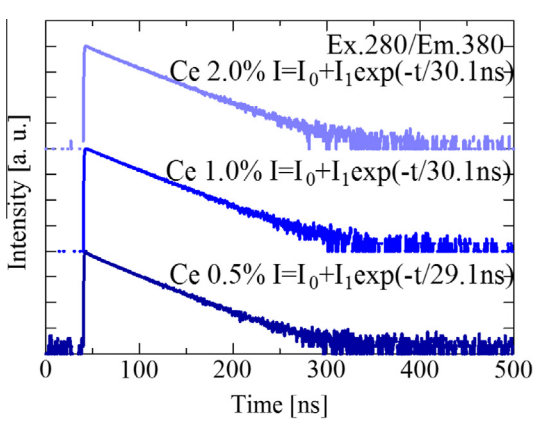

Fig. 3. PL decay time profiles of the Ce:$SrAl_2O_4$ crystals.

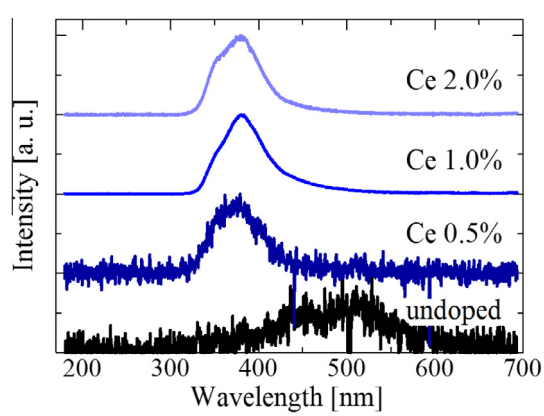

Fig. 5. X-ray induced RL spectra of the Ce:$SrAl_2O_4$ crystals.

some other mechanisms such as exciton [27] or a consecutive capture of electron-hole pairs [28] may affect the deceleration of the scintillation. As the Ce concentration increase, the decay time constants become faster, and it is a common tendency of the rare earth doped scintillators. Ce:$SrAl_2O_4$ has almost the same decay time constant compared to Ce-doped silicate materials [6,7], and the decay time is fast enough for scintillator uses. Due to the low emissivity, we cannot observe the decay time profile of the undoped sample.

Pulse height spectra of the Ce-doped samples measured under ^{137}Cs γ-ray exposure are shown in Fig. 7. The 0.5% Ce:YAG transparent ceramic scintillator [25] was used as a reference which had an absolute light yield of ~20,000 ph/MeV calibrated by using Si-APD and ^{55}Fe source. Only the 1.0% Ce:$SrAl_2O_4$ crystal shows a significantly large signal. Taking into account the quantum

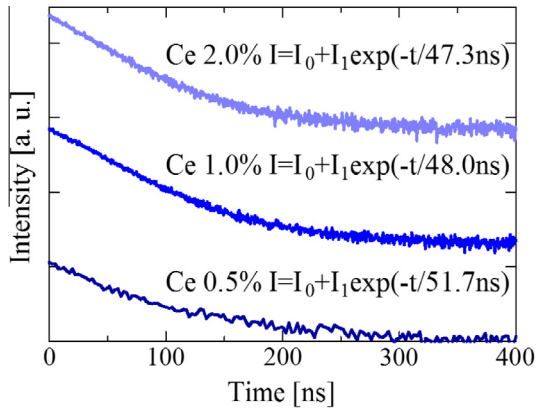

Fig. 6. X-ray induced RL decay time profiles of the Ce:$SrAl_2O_4$ crystals.

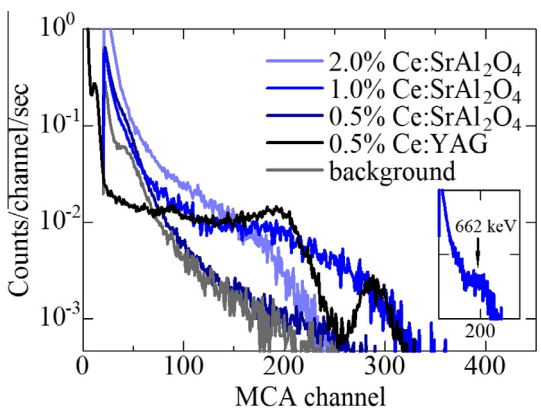

Fig. 7. Pulse height spectra of the Ce:$SrAl_2O_4$ crystals under ^{137}Cs exposure. The inset shows a reduced plot of the 1.0% Ce-doped sample.

efficiency of the PMT and the light yield of Ce:YAG scintillator as a reference, the absolute light yield of the 1.0% Ce-doped $SrAl_2O_4$ is deduced to be ~3900 ph/MeV with a typical error of 10% if we assume ~200 ch corresponds to the full energy deposition. The 2.0% Ce-doped sample shows a smaller light yield, and the 0.5% Ce-doped sample shows only a slightly higher signal than the background. The poor energy resolution would be due to the imperfection of the crystals containing significant amount of cracks. The latter may be due to the charge imbalance of Ce^{3+} and Sr^{2+} in crystals. Compared with the Eu-doped $SrAl_2O_4$ crystals which exhibit ~46,000 ph/MeV [29], scintillation light yield of Ce:$SrAl_2O_4$ is lower. To our experience, we can detect ^{137}Cs signal in the pulse height from only a few% of newly developed crystals, and this result suggests that the matching of energy levels of Ce^{3+} emission center and $SrAl_2O_4$ host is promising. In this point of view, studying a Ba-substituted crystal, $BaAl_2O_4$, as a scintillator is an interesting future assignment since typically alkaline earth aluminate materials show similar luminescence properties.

The afterglow curves of the Ce:$SrAl_2O_4$ crystals by an X-ray irradiation are represented in Fig. 8. Here, the X-ray pulse duration is 2 ms. The afterglow levels of the 0%, 0.5%, 1.0% and 2.0% Ce:$SrAl_2O_4$ crystals are 0.090%, 0.082%, 0.146% and 0.110%, respectively. The 0.5% Ce:$SrAl_2O_4$ crystal shows relatively low afterglow level among the present samples. In these evaluations, after glow levels (A) are defined as $A\ (\%) = 100 \times (I_2 - I_0)/(I_1 - I_0)$ where I_0, I_1 and I_2 denote the averaged signal intensity before the X-ray irradiation, the averaged signal intensity during X-ray irradiation and signal intensity at $t = 20$ ms after the X-ray cut off, respectively. Although the evaluation manners of the afterglow differ by each manufacture, the

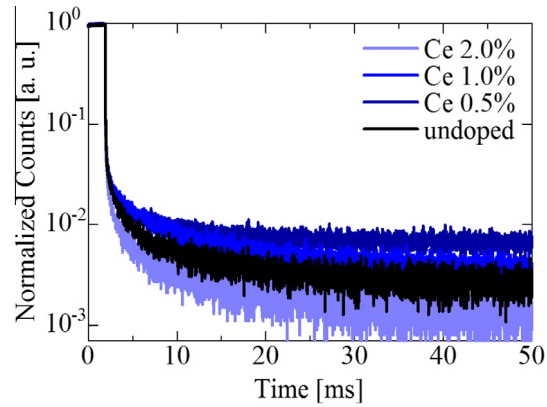

Fig. 8. Afterglow curves of the Ce:$SrAl_2O_4$ crystals.

latter method is the way used by NIHON KESSHO KOGAKU CO., Ltd. which is one of the well-known manufactures of scintillation detectors for medical and security applications. Compared with the afterglow levels of other scintillators used in practice such as $CdWO_4$ and $Bi_4Ge_3O_{12}$ [23], the afterglow levels of our samples are higher.

Fig. 9 shows TSL glow curves of the samples after X-ray exposure of 10 Gy. In the 1.0% Ce-doped sample, TSL glow peaks are observed around 110 and 330 °C. In addition to these peaks, TSL glow peaks around 210 °C appears in the 2.0% Ce-doped sample. These peaks were reported in past studies measured with a powder form of $SrAl_2O_4$ co-doped with Eu-Ce [14] and Ce-Mn [30]. Although the emission origins were not clear in the past studies since they only presented the data of co-doped materials [14,30], the present work clarifies that the Ce-doping plays an important role to generate these glow peaks. In the undoped and 0.5% Ce-doped samples, there are barely measurable emissions. It is suggested that the doping of Ce makes more defects in the $SrAl_2O_4$ possibly due to the charge imbalance of Sr^{2+} and Ce^{3+}. These results are roughly consistent with the afterglow levels (shown in Fig. 8) since afterglow is a type of TSL at room temperature.

The OSL spectra of the Ce:$SrAl_2O_4$ crystals are illustrated in Fig. 10. Here, the samples were irradiated with X-rays of 1.0 Gy. While exposing the samples to the stimulation light at 655 nm, emission bands by Ce^{3+} are observed at the wavelength around 380 nm. The 1.0% Ce-doped sample shows the highest intensity of OSL among the samples, and the undoped sample does not show the OSL signal. Throughout these studies, it is confirmed that Ce:$SrAl_2O_4$ not only works as a scintillator but also works as TSL and

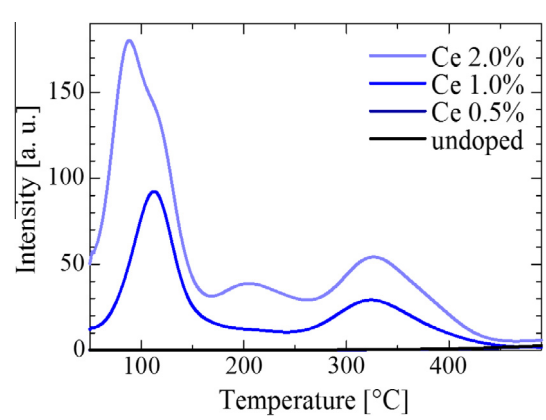

Fig. 9. TSL glow curves of the Ce:$SrAl_2O_4$ crystals after 10 Gy X-ray exposure.

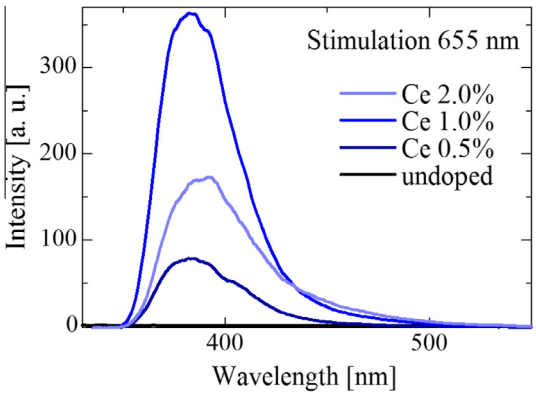

Fig. 10. OSL spectra of the Ce:$SrAl_2O_4$ crystals under 655 nm stimulation.

OSL dosimeters. Therefore, this material system is an interesting candidate to be used for radiation detector applications. It should be pointed out here that for the purpose of dosimeter applications, the effective atomic number (Z_{eff}) of detector materials should be close to that of human issue (Z_{eff} = 7.13). Therefore, Sr substituted compositions such as $MgAl_2O_4$ and $BeAl_2O_4$ would be interesting to investigate in the future.

4. Conclusions

We investigated the optical, scintillation and dosimetric properties of the Ce:$SrAl_2O_4$ crystals prepared by the FZ method. The Ce:$SrAl_2O_4$ crystals show PL and RL peaks due to the 5d-4f transition of Ce^{3+}, and the decay time constants are almost the same as the typical emissions from Ce^{3+} doped phosphors. The *QY* of the 1.0% Ce-doped sample is the highest among the present samples. From pulse height spectra, the light yield of the 1.0% Ce-doped sample is ~3900 ph/MeV. Furthermore, Ce^{3+}:$Sr_2Al_2O_4$ also shows dosimeter properties such as TSL and OSL. The presence of dosimeter properties indicates that the material has a potential to further improve as a scintillator as scintillation and dosimeter properties are understood to be complementally related.

Acknowledgements

This work was supported by a Grant in Aid for Scientific Research (A)-26249147 from the Ministry of Education, Culture, Sports, Science and Technology of the Japanese government (MEXT) and partially by JST A-step. Green Photonics Research from MEXT is also acknowledged. It is also partially supported by the Murata Science Foundation, KRF foundation and a cooperative research project of the Research Institute of Electronics, Shizuoka University.

References

[1] T. Yanagida, A. Yoshikawa, Y. Yokota, K. Kamada, Y. Usuki, S. Yamamoto, M. Miyake, M. Baba, K. Sasaki, M. Ito, Development of Pr: LuAG scintillator array and assembly for positron emission mammography, IEEE Trans. Nucl. Sci. 57 (2010) 1492–1495.
[2] D. Totsuka, T. Yanagida, K. Fukuda, N. Kawaguchi, Y. Fujimoto, Y. Yokota, A. Yoshikawa, Performance test of Si PIN photodiode line scanner for thermal neutron detection, Nucl. Instrum. Methods A 659 (2011) 399–402.
[3] T. Ito, M. Kokubun, T. Takashima, T. Yanagida, S. Hirakuri, R. Miyawaki, H. Takahashi, K. Makishima, T. Tanaka, K. Nakazawa, T. Takahashi, T. Honda, Developments of a new 1-dimensional γ-ray position sensor using scintillators coupled to a Si strip detector, IEEE Trans. Nucl. Sci. 53 (2006) 2983–2990.
[4] C.L. Melcher, Scintillators for well logging applications, Nucl. Instrum. Methods B 40–41 (1989) 1214–1218.
[5] T. Yanagida, K. Fukuda, N. Kawaguchi, S. Kurosawa, Y. Fujimoto, Y. Futami, Y. Yokota, K. Taniue, H. Sekiya, H. Kubo, A. Yoshikawa, T. Tanimori, Scintillation properties of Nd^{3+}, Tm^{3+}, and Er^{3+} doped LuF_3 scintillators in the vacuum ultra violet region, Nucl. Instrum. Methods A 659 (2011) 258–261.
[6] C.L. Melcher, J.S. Schweitzer, Cerium-doped lutetium oxyorthosilicate: a fast, efficient new scintillator, IEEE Trans. Nucl. Sci. 39 (1992) 502–505.
[7] L. Pidol, A. Kahn-Harari, B. Viana, E. Virey, B. Ferrand, P. Dorenbos, J.T.M. de Haas, C.W.E. van Eijk, High efficiency of lutetium silicate scintillators, Ce-doped LPS, and LYSO crystals, IEEE Trans. Nucl. Sci. 51 (2004) 1084–1087.
[8] M.A. Spurrier, P. Szupryczynski, K. Yang, A.A. Carey, C.L. Melcher, Effects of Ca^{2+} Co-doping on the scintillation properties of LSO:Ce, IEEE Trans. Nucl. Sci. 55 (2008) 1178–1182.
[9] K. Takagi, T. Fukazawa, Cerium-activated Gd_2SiO_5 single crystal scintillator, Appl. Phys. Lett. 42 (1983) 43–45.
[10] T. Matsuzawa, Y. Aoki, N. Takeuchi, Y. Murayama, A new long phosphorescent phosphor with high brightness, $SrAl_2O_4$: Eu^{2+}, Dy^{3+}, J. Electrochem. Soc. 143 (1996) 2670–2673.
[11] Z. Fu, S. Zhou, S. Zhang, Study on optical properties of rare-earth ions in nanocrystalline monoclinic $SrAl_2O_4$: Ln (Ln = Ce^{3+}, Pr^{3+}, Tb^{3+}), J. Phys. Chem. B 109 (2005) 14396–14400.
[12] D. Jia, X.-J. Wang, W. Jiad, W.M. Yen, Trapping processes of 5d electrons in Ce^{3+} doped $SrAl_2O_4$, J. Lumin. 122–123 (2007) 311–314.
[13] B.Y. Geng, J.Z. Ma, F.M. Zhan, A solution chemistry approach for one-dimensional needle-like $SrAl_2O_4$ nanostructures with Ln (Ce^{3+}, Eu^{2+} and Tb^{3+}) as activator/dopant, J. Alloys Compd. 473 (2009) 530–533.
[14] X. Xu, Y. Wang, X. Yu, Y. Li, Y. Gong, Investigation of Ce–Mn energy transfer in $SrAl_2O_4$:Ce^{3+}, Mn^{2+}, J. Am. Ceram. Soc. 94 (2011) 160–163.
[15] R. Zheng, L. Xu, W. Qin, J. Chen, B. Dong, L. Zhang, H. Song, Electrospinning preparation and photoluminescence properties of $SrAl_2O_4$:Ce^{3+} nanowires, J. Mater. Sci. 46 (2011) 7517–7524.
[16] P.J.R. Montes, M.E.G. Valerio, G.M. Azevedo, Radioluminescence and X-ray excited optical luminescence of $SrAl_2O_4$: Eu nanopowders, Nucl. Instrum. Methods B 266 (2008) 2923–2927.
[17] R. Meléndrez, O. Arellano-Tánori, M. Pedroza-Montero, W.M. Yen, M. Barboza-Flores, Temperature dependence of persistent luminescence in β-irradiated $SrAl_2O_4$:Eu^{2+}, Dy^{3+} phosphor, J. Lumin. 129 (2009) 679–685.
[18] P.J.R. Montes, M.E.G. Valerio, Radioluminescence properties of rare earths doped $SrAl_2O_4$ nanopowders, J. Lumin. 130 (2010) 1525–1530.
[19] K. Korthout, K. Van den Eeckhout, J. Botterman, S. Nikitenko, D. Poelman, P.F. Smet, Luminescence and x-ray absorption measurements of persistent $SrAl_2O_4$:Eu, Dy powders: evidence for valence state changes, Phys. Rev. B 84 (2011) 085140.
[20] M. Ayvacıklı, A. Ege, N. Can, Radioluminescence of $SrAl_2O_4$:Ln^{3+} (Ln = Eu, Sm, Dy) phosphor ceramic, Opt. Mater. 34 (2011) 138–142.
[21] T. Yanagida, Y. Fujimoto, K. Watanabe, K. Fukuda, N. Kawaguchi, Y. Miyamoto, H. Nanto, Scintillation and optical stimulated luminescence of Ce-doped CaF_2, Radiat. Meas. 71 (2014) 162–165.
[22] T. Yanagida, K. Kamada, Y. Fujimoto, H. Yagi, T. Yanagitani, Comparative study of ceramic and single crystal Ce:GAGG scintillator, Opt. Mater. 35 (2013) 2480–2485.
[23] T. Yanagida, Y. Fujimoto, T. Ito, K. Uchiyama, K. Mori, Development of X-ray-induced afterglow characterization system, Appl. Phys. Exp. 7 (2014) 062401.
[24] T. Yanagida, Y. Fujimoto, N. Kawaguchi, S. Yanagida, Dosimeter properties of AlN, J. Ceram. Soc. Jpn. 121 (2013) 988–991.
[25] T. Yanagida, H. Takahashi, T. Ito, D. Kasama, M. Kokubun, K. Makishima, T. Yanagitani, H. Yagi, T. Shigeta, T. ITO, Evaluation of properties of YAG (Ce) ceramic scintillators, IEEE Trans. Nucl. Sci. 52 (2005) 1836–1841.
[26] D. Nakauchi, G. Okada, M. Koshimizu, T. Yanagida, Optical and scintillation properties of Nd-doped $SrAl_2O_4$ crystals, J. Rare Earths (2016). in press.
[27] R. Visser, P. Dorenbos, C.W.E. van Eijk, A. Meijerink, G. Blasse, H.W. den Hartog, Energy transfer processes involving different luminescence centres in BaF_2:Ce, J. Phys. Condens. Mater. 5 (1993) 1659–1680.
[28] A.J. Wojtowicz, P. Szupryczynski, D. Wisniewski, J. Glodo, W. Drozdowski, Electron traps and scintillation mechanism in $LuAlO_3$:Ce, J. Phys. Condens. Mater. 13 (2001) 9599.
[29] D. Nakauchi, G. Okada, M. Koshimizu, T. Yanagida, Storage luminescence and scintillation properties of Eu-doped $SrAl_2O_4$ crystals, J. Lumin. (2016), http://dx.doi.org/10.1016/j.jlumin.2016.04.008. in press.
[30] T. Katsumata, S. Toyomane, R. Sakai, S. Komuro, T. Morikawa, Trap levels in Eu-doped $SrAl_2O_4$ phosphor crystals co-doped with rare-earth elements, J. Am. Ceram. Soc. 89 (2006) 932–936.